pp 586–599. © Royal Aeronautical Society 2019
doi:10.1017/aer.2019.19

Combustion instability characteristics in a dump combustor using different hydrocarbon fuels

D. Hwang, Y. Song and K. Ahn
kbahn@cbnu.ac.kr
School of Mechanical Engineering
Chungbuk National University
Cheongju, Korea

ABSTRACT

The combustion instability characteristics in a model dump combustor with an exhaust nozzle were experimentally investigated. The first objective was to understand the effects of operating conditions and geometric conditions on combustion instability. The second objective was to examine more generalised parameters that affect the onset of combustion instability. Three different premixed gases consisting of air and hydrocarbon fuels (C_2H_4, C_2H_6, C_3H_8) were burnt in the dump combustor at various inlet velocity, equivalence ratio and combustion chamber length. Dynamic pressure transducer and photomultiplier tube with a bandpass filter were used to measure pressure fluctuation and CH^* chemiluminescence data. Peak frequencies and their maximum power spectral densities of pressure fluctuations at same equivalence ratios showed different trends for each fuel. However, the dynamic combustion characteristics of pressure fluctuations displayed consistent results under similar characteristics chemistry times regardless of the used hydrocarbon fuels. The results showed that characteristic chemistry time and characteristic convection time influenced combustion instabilities. It was found that the convective-acoustic combustion instability could be prevented by increasing the characteristic chemistry time and characteristic convection time.

Keywords: Combustion instability; Dump combustor; Characteristic chemistry time; Characteristic convection time; Dominant frequency; Power spectral density

NOMENCLATURE

RMS root mean square
PSD power spectral density

Received 08 June 2018; revised 15 November 2018; accepted 07 March 2019.

Symbols

c	speed of sound
$CH^{*\prime}$ CH*	chemiluminescence fluctuation
L_C	combustion chamber length
L_I	inlet length
P'	pressure fluctuation
S_L	laminar burning velocity
u	inlet mean velocity
W_I	inlet width
Δx	flame thickness
τ_{acou}	characteristic acoustic time
τ_{chem}	characteristic chemistry time
τ_{conv}	characteristic convection time
τ_{po}	period of pressure oscillation
φ	equivalence ratio

1.0 INTRODUCTION

Dump combustors are widely used in gas turbine engines and ramjet engines due to their suitable geometrical feature for flame stabilisation. Modern gas turbine engines are commonly operated under fuel-lean premixed flames or partially premixed flames to avoid environmental problems[1–3]. Premixed flames in the vicinity of blow-off limit often become unstable. Small temporal perturbations in the fuel-air ratio can considerably influence the heat release rate oscillations. Many researchers also showed that mixing of hot combustion products with fresh reactants by large-scale coherent vortical structures causes periodic heat release patterns, which plays an important role in sustaining combustion instabilities[4–9].

Yu et al.[6] experimentally studied the effects of inlet velocity and inlet/combustor lengths on pressure oscillations in a ramjet combustor. Yoon et al.[10] investigated the relation between inlet velocity and combustion instabilities in a model gas turbine combustor, and suggested that there might be different instability mechanisms under lower and higher velocity conditions. Kim et al.[11] found that combustion instabilities were affected by acoustical coupling of combustor and inlet mixing section geometry. They showed that lower instability frequencies were associated with 1L (longitudinal) mode of the combustor length and higher instability frequencies were related to the 2L mode of the combustor and inlet mixing section. Crump et al.[12] identified four separate longitudinal combustion instabilities in ramjet engines by changing the inlet/combustor geometries and fuels. Taamallah et al.[13] investigated the occurrence of thermo-acoustic instabilities and related it to the mean flame structures under acoustically coupled or decoupled conditions.

Yoon et al.[14] studied the effects of fuel composition on combustion instability frequency and mode shifting in a partially premixed model combustor. They discovered that convection time was the main parameter for combustion instability frequency/mode shifting. Venkataraman et al.[15] showed that the equivalence ratio, inlet velocity, inlet fuel distribution, centerbody recess and swirl influenced combustion stabilities. Their experimental results demonstrated that characterization of flame-flowfield interactions was important in understanding unstable combustion. Park and Lee[16] also researched on combustion instability by varying fuel composition of H_2/CO/CH_4 syngases and synthetic natural gases

https://doi.org/10.1017/aer.2019.19 Published online by Cambridge University Press

in a partially-premixed gas turbine combustor. They suggested that laminar burning velocity, adiabatic flame temperature and ignition delay time should be considered as important parameters to avoid combustion instabilities when designing a gas turbine combustor and deciding operating conditions. Allison et al.[17] investigated the effects of fuel type, flame speed, burner geometry and air flow rate on the instability frequency and amplitude in a dual-swirl burner using different hydrocarbon fuels and syngas. They emphasised on the role of laminar flame speed on the combustion instability.

Unlike the classical thermo-acoustic mode in which the whole system resonates at its natural modes, Yu et al.[6] proposed that instability phenomena with long inlet lengths and relatively short combustor lengths might be considered as a mixed acoustic-convective mode. In their case, the instability mechanism was owing to the coupling of acoustic and convective processes. Vortices were shed periodically from the dump plane and were convected downstream, carrying fresh gases into burned gases. They impinged on the exhaust nozzle after a characteristic convection time ($\tau_{conv} = L_C/u$). At that moment, the fresh gases reacted suddenly and their volumetric expansion generated a pressure wave. The wave induced the shedding of another vortex from the dump plane after a characteristic acoustic time ($\tau_{acou} = 2L_I/c$) which is the round-trip time of the pressure wave travelling up the inlet and back. Thus, the instability frequency satisfied the criterion ($\tau_{conv} + \tau_{acou} = N\tau_{po}$) where N is an integer. Later, Schadow and Gutmark[5] and Samaniego et al.[7] also observed a coupled acoustic-convective mechanism.

Although much experimental and numerical studies have been performed, combustion instability characteristics in a dump combustor with a short length using different hydrocarbon fuels have not been widely investigated. Moreover, it is still impossible to predict whether combustion instability will occur or not in a newly developing engine. The first objective of this study is to investigate how operating conditions (inlet velocity and equivalence ratio of premixed gas with different hydrocarbon fuel) and geometric parameter (combustor length) affect the frequency and amplitude of combustion instabilities. The second objective is to suggest the possibility of the characteristic convection time and chemistry time in predicting combustion instabilities.

2.0 EXPERIMENTAL METHODS

2.1 Experimental set-up

A schematic diagram of a two-dimensional model dump combustor is shown in Fig. 1. The inlet section had cross section of 25 (depth) × 25 (width) mm and length of 360 mm. The combustion chamber section had cross section of 25 (depth) × 75 (width) mm and its length (L_C) could be varied from 75 mm to 125 mm by moving an exhaust nozzle. The opening area of the exhaust nozzle was 25 (depth) × 15 (width) mm. Two quartz windows were attached to the front and back walls so that inside of the chamber section could be viewed. Fuel and air were injected from two opposite sides into the inlet section at 35 mm downstream of the inlet bottom. Choked orifices were used in both the fuel and air supply lines to keep the fuel/air flow rates constant and to prevent any acoustic disturbances in the combustor from affecting the flow rates. A torch ignitor, which used gaseous methane and oxygen, was installed at 40 mm upstream of the chamber dump plane.

A piezoelectric sensor (PCB Piezotronics, 101A05) were flush-mounted at 90 mm upstream of the dump plane. A photomultiplier tube (Thorlabs, PDA100A-EC) with a 431.5 ± 5 nm

https://doi.org/10.1017/aer.2019.19 Published online by Cambridge University Press

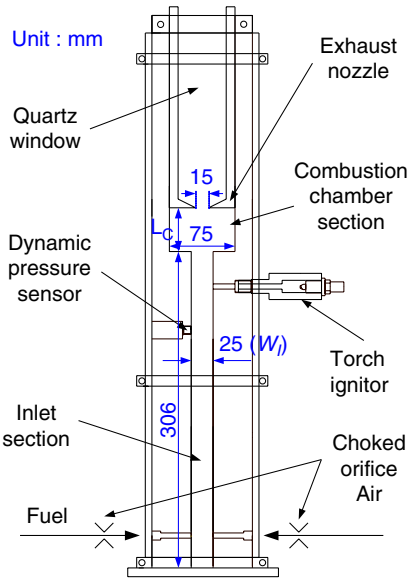

Figure 1. Schematic diagram of the present dump combustor.

bandpass filter was used to detect CH* chemiluminescence intensity from the combustion chamber section between the dump plane and the nozzle. The intensity signals were amplified by a signal conditioner (PCB Piezotronics, 482A16) and recorded at a rate of 10 kHz by a NI c-DAQ. The sampling time for analysing dynamic combustion characteristics was 0.5 second for all tests.

2.2 Experimental conditions

The inlet/combustion chamber lengths, inlet mean velocity, and equivalence ratio are known to influence the flame structure in a dump combustor[6,15,17]. In the current study, hot-firing tests with different fuels (ethylene, ethane, propane) were carried out by independently varying the chamber length, inlet mean velocity, and equivalence ratio. The present experimental conditions are summarised in Table 1. Equivalence ratios for each fuel were differently selected in a range of fuel-lean conditions to examine combustion characteristics under same equivalence ratio or similar characteristic chemistry time between fuels. For the case of ethylene, flashback occurred at $\varphi = 0.75$ depending on the inlet velocity and thus hot-firing tests were performed up to $\varphi = 0.70$.

It is known that the burning velocity and flame thickness change with respect to fuel type, pressure, temperature, and equivalence ratio. Though various fuels were burned with air at same equivalence ratio, their flame structures were dissimilar due to their different chemical reaction rate[18,19]. In order to analyse combustion characteristics with respect to the fuels' chemistry time, the characteristic chemistry time for each fuel was calculated and summarised in Table 2. According to Sterling[20], the characteristic chemistry time is defined as follows:

$$\tau_{chem} = \frac{\triangle x}{S_L} \quad \ldots (1)$$

https://doi.org/10.1017/aer.2019.19 Published online by Cambridge University Press

Table 1
Experimental conditions

Fuel	φ	u [m/s]	L_C [mm]
C_2H_4	0.60 – 0.70	10, 15, 20	75, 100, 125
C_2H_6	0.60 – 0.85	10, 15, 20	75, 100, 125
C_3H_8	0.60 – 0.85	10, 15, 20	75, 100, 125

Table 2
Characteristic chemistry time for each fuel [unit: ms]

φ	C_2H_4	C_2H_6	C_3H_8
0.60	1.511	4.008	4.294
0.65	1.021	2.408	2.615
0.70	0.739	1.622	1.764
0.75		1.182	1.278
0.80		0.911	0.976
0.85		0.732	0.776

Here, the laminar burning velocity and flame thickness of lean ethylene, ethane and propane flames were acquired from the analytical equation suggested by Göttgens et al.[21].

3.0 RESULTS AND DISCUSSION

3.1 Dynamic combustion characteristics

Raw dynamic pressure and CH* chemiluminescence data sampled at 10 kHz were digitally filtered by a bandpass of 30 and 3,000 Hz to eliminate direct current and noise components. Typical filtered data of dynamic pressure and CH* chemiluminescence under hot-firing tests with or without combustion instabilities are shown in Fig. 2(a). Their power spectral densities are also plotted in Fig. 2(b). When the inlet velocity was 10 m/s, the dynamic pressure/CH* chemiluminescence data showed fluctuations in noise-level and displayed no dominant peak frequencies. By contrast, when the inlet velocity was increased to 20 m/s, the dynamic pressure/CH* chemiluminescence data showed periodic in-phase fluctuations with each other and displayed strong peaks around 180 Hz. This indicated that the onset of the combustion instability was affected by operating condition (inlet velocity), and when the combustion instability took place, the dynamic pressure/CH* chemiluminescence data had the same peak frequencies.

To investigate the overall effects of fuel type, inlet velocity, combustion chamber length and equivalence ratio on the dynamic combustion characteristics in the model dump combustor, root-mean-square (RMS) values of filtered pressure fluctuations were calculated and plotted, as shown in Fig. 3. Regardless of the type of fuel or combustion length, as the inlet velocity increased, the RMS values increased due to higher combustion energy power per unit time.

https://doi.org/10.1017/aer.2019.19 Published online by Cambridge University Press

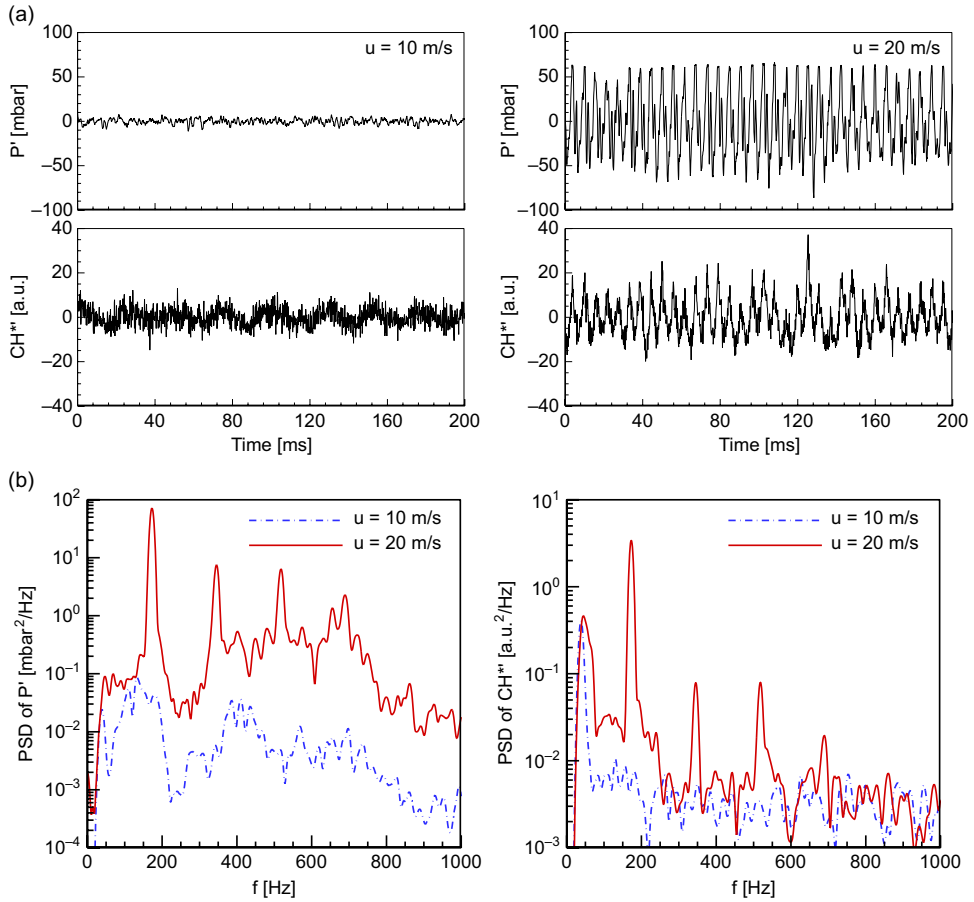

Figure 2. (a) Time histories of the filtered dynamic pressure and CH* chemiluminescence data, and (b) their power spectral densities with C_2H_4 fuel, $\varphi = 0.70$ and $L_C/W_I = 4$.

Other researchers[15,17,22] also observed that as the inlet velocity increased, the pressure fluctuations increased in their combustors. Specifically, Lieuwen[22] found that the inlet velocity was proportional to the maximum normalised pressure amplitude and it played a very significant role in the instability amplitude. As the equivalence ratio increased, in some cases ($u = 15$ and 20 m/s), the RMS values rose almost discontinuously near the equivalence ratio of 0.70. This could be explained by the behavior based on the flame-vortex interaction mechanism that leads to combustion instability. Venkataraman et al.[15] showed that the flame and vortex did not interact at lower equivalence ratios, but at slightly increased equivalence ratios, the flame expanded by higher flame speed could interact with the vortex structure, inducing unstable combustion.

It was possible to find a steep peak in the power spectral density plot when the RMS value of pressure fluctuations was approximately above 10 mbar. In the present study, the RMS value of 10 mbar was thus chosen as a criterion for the onset of combustion instability. At the same inlet velocity and combustor length, the minimum equivalence ratio at which combustion

https://doi.org/10.1017/aer.2019.19 Published online by Cambridge University Press

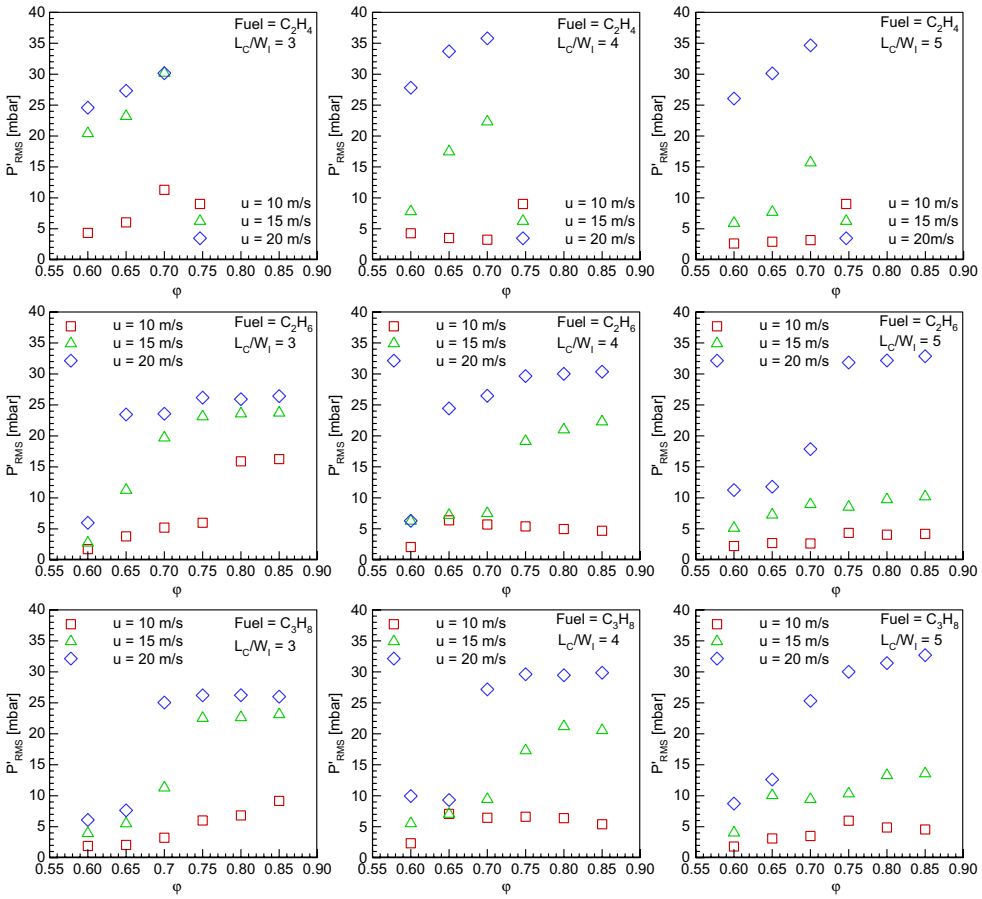

Figure 3. RMS values of the filtered pressure fluctuations under the whole range of experimental conditions.

instabilities took place depended on the fuel type. For cases with $u = 15$ m/s, the amplitudes of pressure fluctuation usually decreased with an increase in the combustor length. These results showed that combustion instabilities in a model dump combustor are greatly affected by fuel type and operating/geometric conditions.

To specifically examine the effects of used fuels on the dynamic combustion characteristics, the peak frequency and maximum power spectral density value for the cases with $u = 15$ m/s and $L_C/W_I = 3$ were obtained. They were plotted as a function of equivalence ratio, as shown in Fig. 4. It is already well-known that as the equivalence ratio increased under fuel-lean conditions, the peak frequency and its power spectral density also increased due to higher combustion temperature (shorter acoustic time) and greater combustion power. However, though the combustion tests for each fuel were done at same equivalence ratio and the adiabatic flame temperatures were not much different, C_2H_4 showed higher peak frequencies and much greater maximum power spectral densities than C_2H_6 or C_3H_8. For $\varphi = 0.60$ and 0.65, C_2H_4 underwent unstable combustion, whereas, C_2H_6 and C_3H_8 underwent relatively stable combustion. This was mainly due to the difference in characteristic chemistry times between

https://doi.org/10.1017/aer.2019.19 Published online by Cambridge University Press

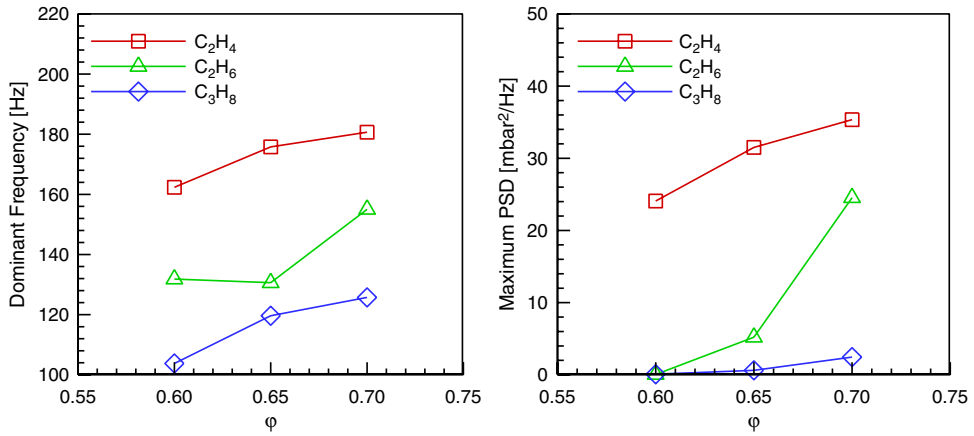

Figure 4. Dominant frequencies and their power spectral densities of the pressure fluctuations at $u = 15$ m/s and $L_C/W_I = 3$.

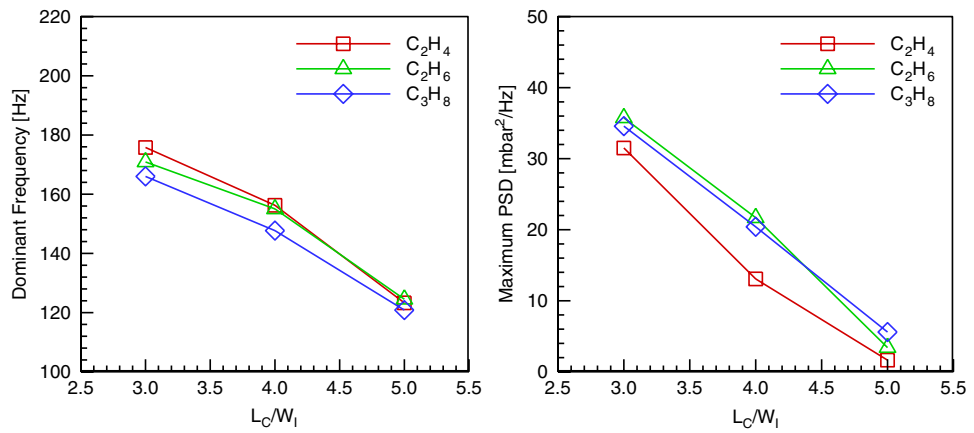

Figure 5. Dominant frequencies and their power spectral densities of the pressure fluctuations for C_2H_4 at $\varphi = 0.65$ ($\tau_{chem} = 1.021$ ms), C_2H_6 at $\varphi = 0.80$ ($\tau_{chem} = 0.911$ ms) and C_3H_8 at $\varphi = 0.80$ ($\tau_{chem} = 0.976$ ms) under $u = 15$ m/s.

the fuel types used. In the next section, therefore, dynamic combustion characteristics were analysed from the viewpoint of characteristic chemistry time.

3.2 Pressure fluctuation characteristics under similar characteristic chemistry times

To study the effects of characteristic chemistry time on dynamic combustion characteristics, the test cases with similar characteristic chemistry times for each fuel were selected. Their peak frequencies and power spectral density values are plotted in Fig. 5 and 6 as a function of normalised combustor length. Though the equivalence ratios for C_2H_4 were lower than those for C_2H_6 and C_3H_8, compared to data in Fig. 4, the results in Figs. 5 and 6 show a very consistent trend regardless of the fuel type. This implied that if characteristic chemistry times

https://doi.org/10.1017/aer.2019.19 Published online by Cambridge University Press

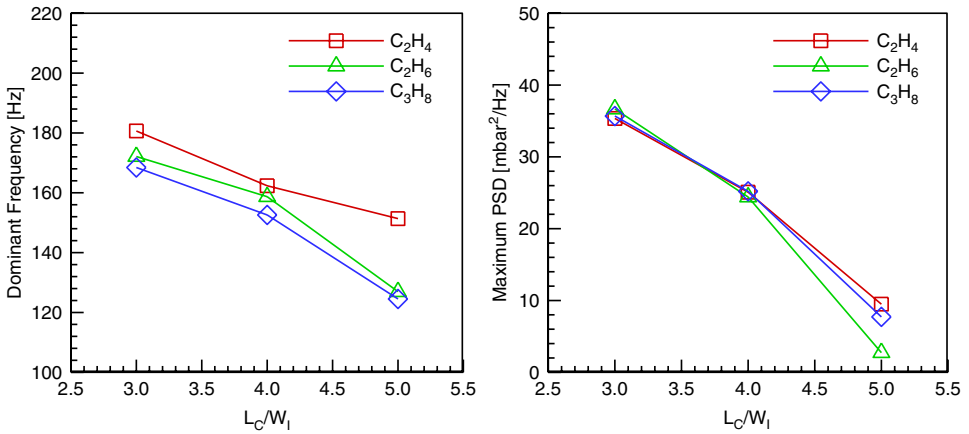

Figure 6. Dominant frequencies and their power spectral densities of the pressure fluctuations for C_2H_4 at $\varphi = 0.70$ ($\tau_{chem} = 0.739$ ms), C_2H_6 at $\varphi = 0.85$ ($\tau_{chem} = 0.732$ ms) and C_3H_8 at $\varphi = 0.85$ ($\tau_{chem} = 0.776$ ms) under $u = 15$ m/s.

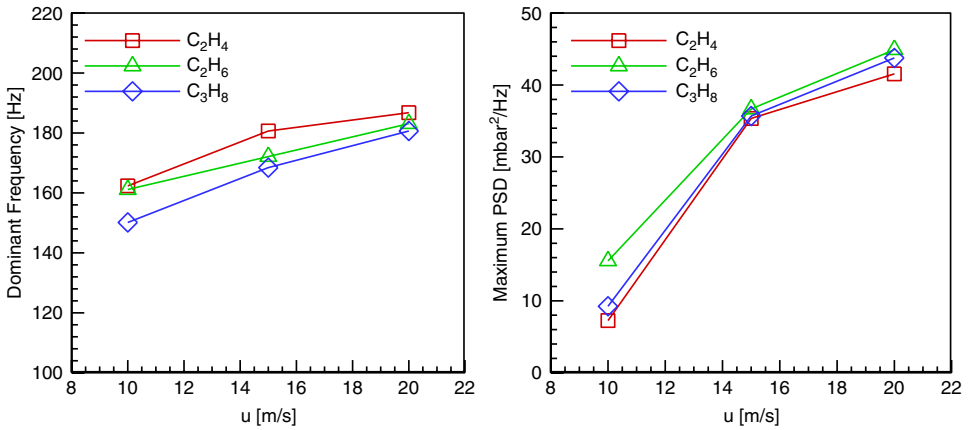

Figure 7. Dominant frequencies and their power spectral densities of the pressure fluctuations for C_2H_4 at $\varphi = 0.70$ ($\tau_{chem} = 0.739$ ms), C_2H_6 at $\varphi = 0.85$ ($\tau_{chem} = 0.732$ ms) and C_3H_8 at $\varphi = 0.85$ ($\tau_{chem} = 0.776$ ms) under $L_C/W_I = 3$.

were similar, hot-firing tests with even different fuels could have similar convective-acoustic combustion instability characteristics.

Figure 7 also presents the experimental results under similar characteristic chemistry times as a function of inlet velocity. Though there were small deviations for each fuel due to slightly different combustion temperature/characteristic chemistry time or measurement errors, the results showed a consistent tendency with respect to the variation in inlet velocity regardless of the fuel type. As the inlet velocity increased, the dominant frequencies and maximum power spectral densities generally increased. The reason for this increase in the dominant frequencies is thought to be the same as that due to the decrease in the combustor length.

From the results provided in Figs. 5, 6 and 7, it was confirmed that the dynamic combustion characteristics of different hydrocarbon fuels in the dump combustor with exhaust nozzle

https://doi.org/10.1017/aer.2019.19 Published online by Cambridge University Press

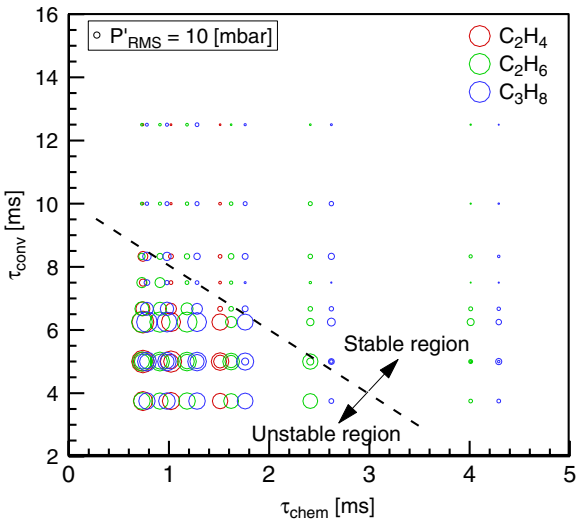

Figure 8. Stability map for combustion instabilities under the whole range of experimental conditions.

could be correlated with the characteristic chemistry time rather than the equivalence ratio. In addition, the results also showed that an increase in the inlet velocity or a decrease in the combustor length raised the probability of unstable combustion with high power spectral densities at dominant frequencies. This implied that the characteristic convection time might play an important role in triggering combustion instabilities.

The RMS values of the filtered pressure fluctuations, as summarised in Fig. 3, are rearranged in Fig. 8 as a function of the characteristic chemistry time and characteristic convection time. Considering P'_{RMS} of 10 mbar as a criterion for the onset of combustion instability, the stability map for the present dump combustor in the whole range of experimental conditions could be approximately obtained as an almost straight line. It was found that as the characteristic chemistry time and characteristic convection time increased, the combustion in the dump combustor became stable.

As Yu et al.[6] and Ahn et al.[23] indicated, the convective-acoustic combustion instability mechanism in the present kind of dump combustor was affected by the relation between vortex shedding and burning. Specifically, Yu et al.[6] found that the resonant frequencies in the convective-acoustic combustion instability are selected according to the following criterion:

$$\frac{1}{4N-1} < \frac{\tau_{conv}}{\tau_{acou}} < \frac{3}{4N-3} \quad \ldots (2)$$

where N is the mode of oscillation. The characteristic acoustic time, which is the feedback time taken for a pressure disturbance to travel up the inlet and back, can be calculated using the inlet length and the sonic velocity in the inlet. The characteristic acoustic time in the present inlet system is 2.12 ms. In the case of $N = 1$, the corresponding characteristic convective time is between 0.71 ms and 6.36 ms, which is well matched with those in the present unstable region. In addition, an increase in the characteristic convection time caused the heat release to be spatially and temporally distributed so that not much return would be transferred to the acoustic field. When the vortical structure impinged the exhaust nozzle, reactants with long characteristic chemistry time would escape through the nozzle without rapid burning.

https://doi.org/10.1017/aer.2019.19 Published online by Cambridge University Press

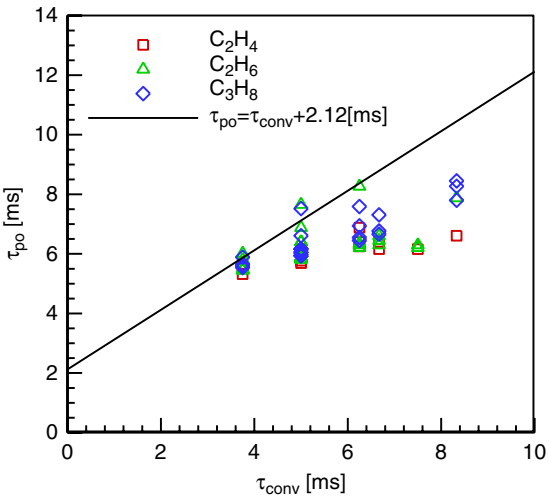

Figure 9. Measured period of pressure oscillation as a function of the characteristic convection time.

These phenomena could explain the effects of characteristic chemistry time and characteristic convection time on the present stability map.

The whole premise of the present work was based on the low time scales of convection and chemistry, thus enabling excitation of sound as evidenced from Fig. 8. However, there was disparity in the two time scales, with the convective time scale being greater than the reaction time scale. This presents a situation whereby, the reaction gets completed before the vortex impinges the wall, which in-turn cannot excite the combustor, owing to lack of significant heat release rate fluctuations. Nevertheless, the combustor was unstable. This seeming contradiction could be explained by considering the shortening of convective time scales, owing to flow acceleration past the flame as well as the role of buoyancy in accelerating the flow.

According to Yu et al.[8], the period of pressure oscillations (τ_{po}, a reciprocal of the dominant frequency) is the sum of the convection time and the acoustic time. To identify the dominant flow/coherent structure causing the acoustics, measured period of pressure oscillations with P'_{RMS} over 10 mbar as is plotted in Fig. 9 as a function of the characteristic convection time. The measured period increases proportionally with the convection time and roughly follows the calculated line. When the convection time is in the vicinity of 4 ms, the measured period is in good agreement with the calculated value. When the convection time exceeds 4 ms, however, the measured period is generally lower than the calculated value. This is probably due to the reduction of the actual convection time mentioned in the previous paragraph.

3.3 CH* Chemiluminescence characteristics under similar characteristic chemistry Times

Global CH* chemiluminescence data in the combustion chamber was measured by a photomultiplier tube with bandpass filter to study heat release fluctuations. The emission of CH radical, which was one of the product generated out of the combustion process, has been successfully used to investigate the heat release fluctuations and flame structures[24–26]. Figure 10 presents the power spectral densities of CH* chemiluminescence data corresponding to the cases in Figs. 5 and 6. The CH* chemiluminescence data displayed identical peak frequencies

https://doi.org/10.1017/aer.2019.19 Published online by Cambridge University Press

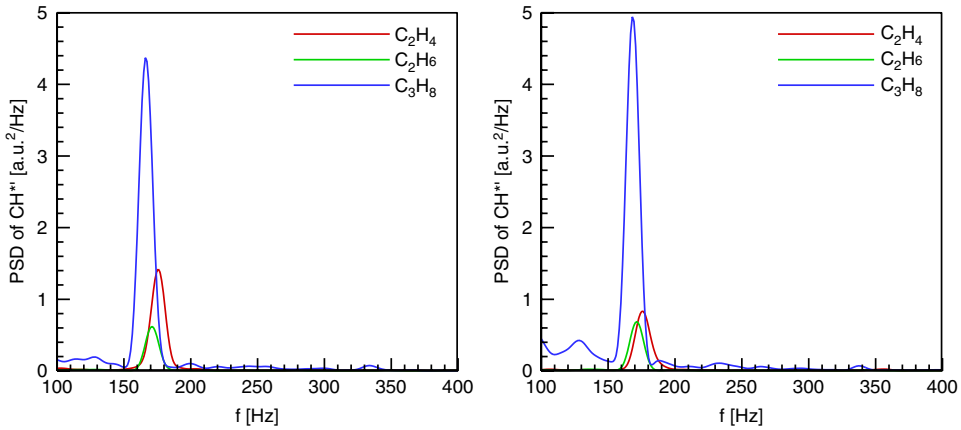

Figure 10. Power spectral densities of the CH* chemiluminescence fluctuations for (a) C_2H_4 at $\varphi = 0.65$, C_2H_6 at $\varphi = 0.80$, C_3H_8 at $\varphi = 0.80$ and (b) C_2H_4 at $\varphi = 0.70$, C_2H_6 at $\varphi = 0.85$, C_3H_8 at $\varphi = 0.85$ under $L_C/W_I = 3$.

with those of the filtered pressure fluctuations. However, the maximum power spectral densities in CH* chemiluminescence data were much different for each fuel and the CH* emission fluctuations in C_3H_8 were significantly higher than the other fuels, although their pressure fluctuations were almost the same. The discrepancy could be due to the emission of CO_2* radicals in the emission range of CH*, specifically at high equivalence ratios that are mapped for C_2H_6 and C_3H_8, which is not seen of C_2H_4 due to low equivalence ratio. The exceedingly large CH* emission fluctuations for C_3H_8 might be a result of higher CO_2 production per mole of combustion. Therefore, amplitude of CH* chemiluminescence data can't be used to estimate the strength of combustion instabilities.

4.0 CONCLUSIONS

An experimental study was carried out to study the dynamic combustion characteristics in dump combustor with exhaust nozzle. To investigate the effects of fuel type, operating conditions and geometric condition on combustion instability characteristics, three different premixed gases composed of air and hydrocarbon fuels (C_2H_4, C_2H_6, C_3H_8) were burned in fuel-lean conditions. The inlet velocity was varied from 10m/s to 20m/s and the equivalence ratio were between 0.60 and 0.85. The combustor length was also changed from 75mm to 125mm.

When the RMS values of the filtered pressure fluctuations were above 10 mbar, the dynamic pressure/CH* chemiluminescence data showed periodic in-phase fluctuations and strong peaks between 160Hz and 180Hz. For the cases with $u = 15$ m/s and $L_C/W_I = 3$ at same equivalence ratios, the pressure fluctuations using C_2H_4 had higher peak frequencies and much greater maximum power spectral densities than those using C_2H_6 or C_3H_8. The RMS values of pressure fluctuations under the same operating conditions and geometric condition showed different results for used fuels. However, the peak frequencies and maximum power spectral densities of the pressure fluctuations at same inlet velocity and combustor length were consistent under similar characteristic chemistry times regardless of fuel type. It was found that the stability map for the present dump combustor could be expressed by

https://doi.org/10.1017/aer.2019.19 Published online by Cambridge University Press

the characteristic chemistry time and characteristic convection time. These clearly shed new insight into the importance of the characteristic chemistry time and characteristic convection time on the onset of combustion instabilities. In light of these findings, if one knows the combustion instability characteristics of a specific hydrocarbon fuel in a dump combustor and the characteristic chemistry time of the fuels, one will be able to predict the peak frequency and amplitude of combustion instabilities using other hydrocarbon fuels. However, more general validity of the results using other gas fuels with a very low/high reactivity or liquid fuels is highly recommended to achieve a deeper understanding.

ACKNOWLEDGEMENTS

This research was supported by the National Research Foundation (NRF-2013R1A5A1073861, NRF-2017R1A1A1A05001237, and NRF-2018M1A3A3A02065683) funded by the Ministry of Science and ICT, South Korea. The authors would like to thank the MSIT for its support.

REFERENCES

1. LEFEBVRE, A.W. Lean premixed/prevaporized combustion, NASA CP-2016, January 1977.
2. FOGLESONG, R.E., FRAZIER, T.R., FLAMAND, L.M., PETER, J.E. and LUCHT, R.P. Flame structure and emissions characteristics of a lean premixed gas turbine combustor, 35th Joint Propulsion Conference and Exhibit, AIAA 1999-2399, Los Angeles, CA, 1999.
3. TACHIBANA, S., ZIMMER, L., KUROSAWA, Y. and SUZUKI, K. Active control of combustion oscillations in a lean premixed combustor by secondary fuel injection coupling with chemiluminescence imaging technique, *Proc Combust Inst*, 2007, **31**, (2), pp 3225–3233.
4. POINSOT, T.J., TROUVE, A.C., VEYNANTE, D.P., CANDEL, S.M. and ESPOSITO, E.J. Vortex-driven acoustically coupled combustion instabilities, *J Fluid Mech*, 1987, **177**, pp 265–292.
5. SCHADOW, K.C. and GUTMARK, E. Combustion instability related to vortex shedding in dump combustors and their passive control, *Prog Energy Combust Sci*, 1992, **18**, (2), pp 117–132.
6. YU, K.H., TROUVE, A. and DAILY, J.W. Low-frequency pressure oscillations in a model ramjet combustor, *J Fluid Mech*, 1991, **232**, pp 47–72.
7. SAMANIEGO, J.M., YIP, B., POINSOT, T. and CANDEL, S. Low-frequency combustion instability mechanisms in a side-dump combustor, *Combust Flame*, 1993, **94**, (4), pp 363–380.
8. GUTMARK, E., SCHADOW, K.C., SIVASEGARAM, S. and WHITELAW, J.H. Interaction between fluid-dynamic and acoustic instabilities in combusting flows within ducts, *Combust Sci Technol*, 1991, **79**, (1–3), pp 161–166.
9. STERLING, J.D. and ZUKOSKI, E.E. Longitudinal mode combustion instabilities in a dump combustor, 25th AIAA Aerospace Sciences Meeting, AIAA 1987-0220, Reno, NV, 1987.
10. YOON, J., KIM, M.K., HWANG, J., LEE, J. and YOON, Y. Effect of fuel-air mixture velocity on combustion instability of a model gas turbine combustor, *Appl Therm Eng*, 2013, **54**, (1), pp 92–101.
11. KIM, M.K., YOON, J., OH, J., LEE, J. and YOON, Y. An experimental study of fuel-air mixing section on unstable combustion in a dump combustor, *Appl Therm Eng*, 2014, **62**, (2), pp 662–670.
12. CRUMP, J.E., SCHADOW, K.C., YANG, V. and CULICK, F.E.C. Longitudinal combustion instabilities in ramjet engines: identification of acoustic modes, *J Propul Power*, 1986, **2**, (2), pp 105–109.
13. TAAMALLAH, S., LABRY, Z.A., SHANBHOGUE, S.J. and GHONIEM, A.F. Thermo-acoustic instabilities in lean premixed swirl-stabilized combustion and their link to acoustically coupled and decoupled flame macrostructures, *Proc Combust Inst*, 2015, **35**, (3), pp 3273–3282.
14. YOON, J., JOO, S., KIM, J., LEE, M.C., LEE, J.G. and YOON, Y. Effects of convection time on the high harmonic combustion instability in a partially premixed combustor, *Proc Combust Inst*, 2017, **36**, (3), pp 3753–3761.
15. VENKATARAMAN, K.K., PRESTON, L.H., SIMONS, D.W., LEE, B.J., LEE, J.G. and SANTAVICCA, D.A., Mechanism of combustion instability in a lean premixed dump combustor, *J Propul Power*, 1999, **15**, (6), pp 909–918.

https://doi.org/10.1017/aer.2019.19 Published online by Cambridge University Press

16. PARK, J. and LEE, M.C. Combustion instability characteristics of H_2/CO/CH_4 syngases and synthetic natural gases in a partially-premixed gas turbine combustor: Part I-frequency and mode analysis, *Int J Hydrogen Energy*, 2016, **41**, (18), pp 7484–7493.
17. ALLISON, P.M., DRISCOLL, J.F. and IHME, M. Acoustic characterization of a partially premixed gas turbine model combustor: syngas and hydrocarbon fuel comparisons, *Proc Combust Inst*, 2013, **34**, (2), pp 3145–3153.
18. AHN, K. and YU, K.H. Effects of Damköhler number on vortex-flame interaction, *Combust Flame*, 2012, **159**, (2), pp 686–696.
19. HWANG, D. and AHN, K. A study on heat release fluctuation using various hydrocarbon fuels, *J Korean Soc Propul Eng*, 2016, **20**, (6), pp 1–10.
20. STERLING, J.D. *Longitudinal mode combustion instabilities in air breathing engines*, California Institute of Technology, 1987, Pasadena, C.A, USA.
21. GÖTTGENS, J., MAUSS, F. and PETERS, N. Analytic approximations of burning velocities and flame thicknesses of lean hydrogen, methane, ethylene, ethane, acetylene and propane flames, *Proc Combust Inst*, 1992, **24**, (1), pp 129–135.
22. LIEUWEN, T.C. Experimental investigation of limit-cycle oscillations in an unstable gas turbine combustor, *J Propul Power*, 2002, **18**, (1), pp 61–67.
23. AHN, K., YU, K. and YOON, Y. Experimental study on combustion instability in a dump combustor, *J Korean Soc Aeronautl Space Sci*, 2006, **34**, (12), pp 35–40.
24. HURLE, I.R., PRICE, R.B., SUGDEN, T.M. and THOMAS, A. Sound emission from open turbulent premixed flames, *Proc Royal Soc A*, 1968, **303**, pp 409–427.
25. LANGHORNE, P.J. Reheat buzz: an acoustically coupled combustion instability. Part 1. experiment, *J Fluid Mech*, 1988, **193**, pp 417–443.
26. ALTAY, H.M., SPETH, R.L., HUDGINS, D.E. and GHONIEM, A.F. The impact of equivalence ratio oscillations on combustion dynamics in a backward-facing step combustor, *Combust Flame*, 2009, **156**, (11), pp 2106–2116.

https://doi.org/10.1017/aer.2019.19 Published online by Cambridge University Press